Simulation-based Performance Evaluation of Mobile Ad Hoc Routing Protocols in a Swarm of Unmanned Aerial Vehicles

M. T. Hyland
mhyland@afit.edu

B. E. Mullins
Senior Member, IEEE
bmullins@afit.edu

R. O. Baldwin
Senior Member, IEEE
rbaldwin@afit.edu

M. A. Temple
Senior Member, IEEE
mtemple@afit.edu

Abstract

This paper evaluates the performance of several ad hoc routing protocols in the context of a swarm of autonomous unmanned aerial vehicles (UAVs). It has been proposed that a wireless network where nodes have on average 5.1774 log n neighbors, where n is the total number of network nodes, has a high probability of having no partitions. By decreasing transmission range and implementing multi-hop routing between nodes, while ensuring network connectivity is maintained, spatial multiplexing of the wireless channel is exploited. The proposed process is evaluated using the OPNET network simulation tool for the Greedy Perimeter Stateless Routing (GPSR), Optimized Link State Routing (OLSR), and Ad hoc On-demand Distance Vector (AODV) routing protocols in the context of a swarm of UAVs.

1. Introduction

A proposed swarm of autonomous and semi-autonomous unmanned aerial vehicles (UAVs), called a "Host of Armed Reconnaissance Vehicles Enabling Surveillance and Targeting" (HARVEST), includes heterogeneous unmanned aircraft with varying capabilities collaborating to accomplish a common objective [1]. A variety of sensor UAVs collect various data about potential targets and route pertinent reconnaissance and control information to and from ground or air-based decision-makers through edge access UAVs. Another application of networked autonomous UAVs is a cooperative search system presented in [2] and [3] where a swarm of UAVs search and monitor the ground for enemy targets, adaptively collaborating to complete the objective in less time than an uncoordinated effort would require.

To achieve this degree of collaboration, a collection of unmanned vehicles requires effective and efficient communication within the swarm and to external control points. Sensor platforms must be inexpensive, small, and light. To minimize power consumption and maximize loiter time, radio transmission power is necessarily limited. As such, the swarm employs a system to relay data from one node to another by forming a mobile ad hoc wireless network (MANET).

A wide variety of ad hoc routing protocols have been proposed which relay data as required by HARVEST; this paper evaluates several protocols to determine which is most appropriate for use in a HARVEST swarm.

The rest of this paper is organized as follows: Section 2 discusses various routing strategies, the GPSR Protocol, and the impact of transmission range on wireless network connectivity. In Section 3, the simulation environment used in this study is described. Experimental methodology is presented in Section 4 with results presented in Section 5. Section 6 provides conclusions and recommendations for future research.

2. Background

The simplest possible routing protocol relays packets across a network by flooding every packet to every node. In such a broadcast flooding protocol, every unique packet received by every node is retransmitted. Packets are sequenced by the sender to allow nodes to identify packets which have already been rebroadcast. Proving that packets will reach every connected node is trivial and every packet is retransmitted by every node in the network regardless of whether or not retransmission is beneficial. This severely limits available bandwidth as the number of nodes increases. Ad hoc routing protocols attempt to mitigate this problem by determining an efficient routing path in the context of a (potentially) highly-connected wireless network.

One approach to delivering data across a swarm of mobile nodes is to simply increase the transmission power at every node so transmissions can be directly received by every node in the network. Aside from the issue of limited power, this scheme precludes the

21st International Conference on
Advanced Information Networking and Applications Workshops (AINAW'07)
0-7695-2847-3/07 $20.00 © 2007 IEEE

exploitation of "spatial multiplexing," whereby many pairs of nodes communicate using the same transmission channel when the distance between each of the pairs is large enough to prevent interference.

Although the shorter transmission range requires multiple transmissions of the same data packet to relay it from source to destination, it is hypothesized that the corresponding increase in network throughput due to spatial multiplexing will compensate for the redundant transmissions.

Since packets are retransmitted, potentially several times, the time from packet origination at the source to delivery at the destination is necessarily increased. This increase is the "cost" of achieving higher network throughput, and it is hypothesized that a significant increase in network throughput can be achieved with an acceptable increase in end-to-end delay.

Ad hoc routing protocols are typically categorized as either proactive or reactive protocols. Proactive ad hoc protocols maintain routing information for all possible destinations at all times and offer the shortest delay at transmission time. Reactive protocols compute routes as needed which introduces an additional delay before transmission. The trade-off is usually a higher amount of control traffic required by proactive protocols.

This paper describes a robust network simulation platform which evaluates various network components and protocols in the context of a UAV swarm under a variety of network conditions.

2.1 Location-based Routing

In location-based routing protocols, forwarding decisions are based on the relative location of the destination rather than a topology-based route. Since there is no need for the network to maintain route information, location-based routing protocols scale well even in highly mobile networks [4].

Such a routing scheme could be useful in a UAV swarm to deliver data to a location that is known to have connectivity to the network edge for transmission to a ground station. A survey of several location-based routing protocols can be found in [4].

In mobile networks, location-based routing is difficult if nodes do not know the geographic location of every other node in the network. In a UAV swarm, however, every node knows its location via GPS; by including source location in the packet header, the locations of neighboring UAV can be learned over time. Location records at each node can be time stamped and discarded after an expiration period based on node mobility. Furthermore, in many instances data may not necessarily be destined for a specific node, but rather to any node located at or near a specific location. Geographic routing supports this type of addressing scheme while address-based routing protocols cannot.

2.2 Greedy Perimeter Stateless Routing

A location-based reactive ad hoc routing protocol, Greedy Perimeter Stateless Routing (GPSR) [5] forwards packets to the neighboring node geographically closest to the destination.

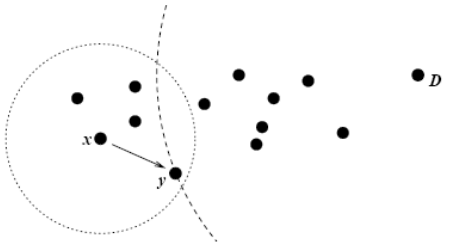

Figure 1. Greedy forwarding example [5]

In Figure 1, node *y* is *x*'s neighbor closest to *D*. The dotted circle represents *x*'s transmission range, while the dashed line is a segment of a circle centered at *D* with radius equal to the distance from *y* to *D*. Any nodes inside the intersection of the two circles would be closer to *D* than *y*. Successive greedy forwarding hops are made until the packet reaches the destination.

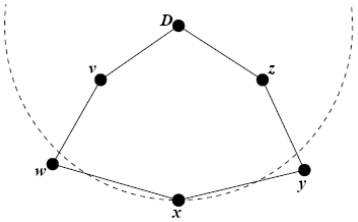

Figure 2. Greedy forwarding failure [5]

Greedy forwarding fails, however, when none of *x*'s neighbors are closer to *D* than *x* as seen in Figure 2. When this occurs, packets must be sent further away from *D* until a node closer to *D* is reached.

Figure 2 clearly shows a path from *x* to *D*; GPSR incorporates an algorithm that finds and exploits such paths called perimeter routing. To accomplish perimeter routing, each GPSR node maintains a planar graph representation of all nodes within its transmission range. However, in a planar graph, no edges cross while a graph representation of a wireless network certainly has crossing edges. GPSR, therefore, uses a planarization algorithm to reduce the full network graph such that the graph remains connected during the reduction. While GPSR could

21st International Conference on
Advanced Information Networking and Applications Workshops (AINAW'07)
0-7695-2847-3/07 $20.00 © 2007 IEEE

use any planarization algorithm that prevents partitions, the Relative Neighborhood Graph (RNG) [6] is used.

Construction of the RNG is depicted in Figure 3. First, the full network graph is created, representing each node as a vertex in the graph and adding edges between each pair of nodes capable of communicating with each other.

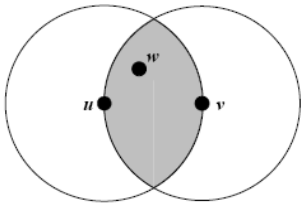

Figure 3. Constructing the RNG [5]

During planarization, every edge is considered for removal. For an edge (u,v) to be included in the RNG, the shaded area must not contain any witness w. Connectivity is ensured since the path (u-v) is replaced by (u-w, w-v).

Table 1. Required Perimeter Mode Data

Item	Description
D	Destination Location
L_p	Location packet entered perimeter mode
L_f	Location on src-dest line packet entered current face
$e0$	First edge traversed on current face
M	Packet Mode (Perimeter or Greedy)

Table 1 lists the data required for each packet in perimeter routing mode. Once a planar representation of the network is computed, a packet that reaches a node without greedy neighbors enters perimeter routing mode. In perimeter routing, the packet is marked for perimeter mode and the L_p field in the packet header is set to the location where the packet first entered perimeter routing mode. The packet is forwarded around the perimeter of the RNG face using the right-hand rule, beginning with the first edge counterclockwise about that node from the line formed by that node and the destination node.

The right-hand rule ensures the packet will be forwarded along the first edge encountered by sweeping counter-clockwise from the incoming edge the packet was received on. An example of perimeter forwarding is shown in Figure 4.

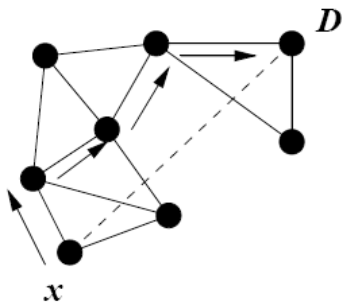

Figure 4. Perimeter forwarding example [5]

If the edge selected by the right-hand rule for forwarding crosses the line between L_f and D, the node records the intersection point into L_f and begins routing around the adjacent face of the planar graph using the right-hand rule. If a packet travels completely around a face and traverses the same edge for a second time without intersecting the line between L_f and D at a point closer to D than L_f, the destination node is disconnected from the graph. GPSR stores the addresses of each node on this first edge in the packet's $e0$ field to detect a loop and discards packets that are addressed to unreachable destinations.

A packet can leave perimeter mode if it reaches a node which is closer to the destination than L_p. A node receiving a perimeter-mode packet compares its current location to L_p and returns the packet to greedy mode if it is closer to the destination node. It is possible, however, that while that node is closer to the destination than L_p, no greedy next hop exists, so the packet could be placed back into perimeter mode.

Note that each node need only determine the RNG which includes those nodes within its transmission range. To do so, it needs to know the existence and location of each of its neighbors. Including location information in every transmitted packet and periodically broadcasting beacon packets containing location information in the absence of data packets, ensures that nodes have the neighbor information necessary to form the local RNG.

2.3 Wireless Network Connectivity

Our hypothesis that it is possible to increase total usable network throughput by exploiting spatial multiplexing is supported by Gupta and Kumar [7]. They conclude the throughput available to each node diminishes to zero as the number of connected nodes increases. To maximize throughput, transmission range is limited to the minimum needed for a connected network.

Xue and Kumar [8] determined that the minimum number of neighbors in a wireless network to ensure connectivity is bounded above by 5.1774 log n, where

n total nodes are present. In a less-connected network, there is a high probability of a partition. In a more-connected network, contention for the medium among more nodes decreases total throughput. Thus, the optimal transmission range in a network of randomly located nodes which has a low probability of network partition can be found by

$$\frac{\pi r^2}{A} = \frac{x}{n} \quad (1)$$

where r is the transmission range in meters, A is the network area in meters squared, x is the number of connected nodes, and n is the total number of nodes.

With a network of uniformly distributed nodes, the ratio of reachable transmission space to the entire network area is proportional to the ratio of the number of immediate neighbors to the total number of nodes. Substituting the desired minimum number of neighbors and solving (1) for r gives

$$r = \sqrt{\frac{xA}{\pi n}} \le \sqrt{\frac{5.1774 A \log n}{\pi n}} \quad (2)$$

A simple Java simulation was used to generate random node configurations and validate the model presented above. Results in Figure 5 with 95% confidence intervals show an excellent agreement between the (2) and the simulation.

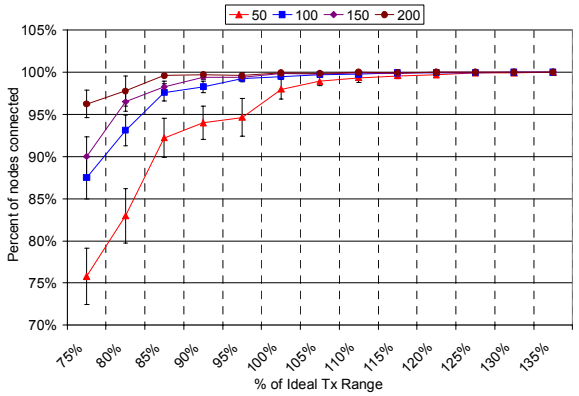

Figure 5. Optimal transmission range results

3. Simulation Environment

Simulation of the UAV swarm is done using OPNET Modeler 12.0.A network simulation software. The *manet_station_adv* standard node model included with OPNET is customized to perform GPSR forwarding capabilities. Networks of 50, 100, 150 and 200 nodes are constructed in a square 10×10 *km* project space.

A custom-built *gpsr_rte* process model contains all GPSR-specific logic and is launched by a modified version of the *ip_dispatch* process via the *manet_mgr* child process in the same manner in which the built-in reactive MANET routing protocols are interfaced.

Random waypoint mobility is used with a zero pause time and a constant travel speed of 25 *m/sec* to simulate UAVs. Simulations are 1,200 *secs* long with 200 *secs* of execution before statistics are collected to randomize node location.

Beacons are randomly transmitted to prevent collisions with beacons from neighbors and are scheduled using self-interrupts chosen from [0.5, 1.5] *secs*.

All packets are IPv4 formatted packets with GPSR data stored in the options field of the IP header. For space efficiency, location coordinates are stored as a pair of 2-byte unsigned integers. The network space is divided along the x and y axis into 2^{16} segments which provides 15 *cm* resolution in defining a location with a 10×10 *km* network boundary.

The 16 least significant bits of the IP addresses of the two nodes on the edge are used to identify *e0*. Using only 16 bits for these fields restricts this implementation to a maximum of 65,534 nodes. The GPSR data packet fields, their size, and the packet modes which use them are shown in Table 2.

Table 2. GPSR Packet Fields

	Field	Bytes	Description
All Packets	Mode	1	packet mode
	sndr_x	2	*x* position of last-hop node
	sndr_y	2	*y* position of last-hop node
Greedy & Perimeter	last_hop	4	IP address of last-hop node
	dest_x	2	*x* position of dest node
	dest_y	2	*y* position of dest node
Perimeter	Lp_x	2	*x* & *y* position of location
	Lp_y	2	pkt entered perimeter mode
	Lf_x	2	*x* & *y* coord of intersection
	Lf_y	2	between current & pev face
	e0_a	2	last 16 bits of IP addr of
	e0_b	2	1st & 2nd node on edge *e0*

Each of eight traffic-generating nodes generates packets with exponentially distributed sizes having a 1024-byte mean and Poisson arrivals. Configurations of 2, 4, 8, 10 and 20 packets per second (*pkts/sec*) are simulated to evaluate performance under various workloads. Each transmitting node chooses a destination node at random at simulation start and transmits packets to that destination for the duration of the simulation. Each time a data packet is generated, the beacon self interrupt is cancelled and rescheduled since beacon information is included in the data packet header. Destination location information is obtained from a central location database as described in [5].

Database lookups are instantaneous and location data is updated by each node at the same rate as beacon packet transmission.

The standard OPNET WLAN transceiver pipeline models are used, and all WLAN configuration attributes are left at their default values with the following exceptions: *Packet Reception-Power Threshold* is set to -90 *dBm*; *RTS Threshold (bytes)* is set to *None*; *Transmit Power* is set at simulation time to vary approximate radio transmission range.

The *wlan_mac* process model is modified to extend interframe spaces to permit longer propagation times and longer transmission distances; the original and modified values are shown in Table 3. The modified slot time is approximately equal to the one-way propagation time for the signal to travel 15 *km*.

Table 3. Modifications to 802.11b Timing

Parameter	802.11 Value	Modified Value
Slot Time	20 μs	50 μs
SIFS	10 μs	28 μs
DIFS	50 μs	128 μs

MAC filtering is disabled so all overheard data frames are passed up the protocol stack and GPSR can learn location information about its neighbors every time a data packet is received, even if it is not addressed to that node.

Upon receiving a packet from IP, GPSR updates the neighbor table. The neighbor table consists of the node address, x and y location coordinates, and the simulation time that the record was added or updated. Location data is considered expired if it has not been updated for a period of time three times as long as the beacon interval or 4.5 *sec*. Beacon packets and overheard data packets are discarded after this step.

If the receiving node is not the intended destination, the packet must be forwarded. At this time, the neighbor table is parsed and expired entries are deleted, after which the distance between every node in the table and the destination location is calculated. The packet is forwarded to the neighbor closest to the destination. If no neighbor is closer than the current node, the packet has reached a "dead end" and the packet is placed in perimeter mode.

A perimeter mode packet is returned to greedy forwarding if the receiving node's location is closer to the destination than the point L_p where it was placed into perimeter mode. Otherwise, the node generates a planar representation of all neighboring nodes and forwards the packet to the next hop according to the right-hand rule described in Section 2. If the next hop would route the packet across the line between L_f and the destination, L_f is updated to the new intersection point, and the next hop is recalculated for the adjacent face in the planar graph.

If the next hop node would cause the packet to traverse the same edge that it did when it first began routing around the current face (identified by the last 16 bits of the IP address of the two nodes on that edge stored in the packet *e0* fields) the destination is truly unreachable and the packet is discarded.

GPSR optimizations that incorporate MAC-layer feedback [5] are not implemented at this time.

4. Methodology

As the OPNET wireless models do not specify transmission range directly, the appropriate model attributes which approximate the desired transmission ranges need to be determined. The two attributes that most directly impact transmission range are *Transmit Power* (*W*) and *Packet Reception-Power Threshold* (*dBm*). The OPNET Modeler documentation provides an approximation for received power P_{rx} given by

$$P_{rx} = P_{tx} \times G_{tx} \times \frac{\lambda^2}{16\pi^2 r^2} \times G_{rx} \quad (W) \tag{3}$$

where P_{tx} is transmit power (*W*), G_{tx} and G_{rx} are the absolute transmit and receive antenna gains, respectively, λ is carrier frequency wavelength (*m*), and r is the distance between transmit and receive nodes (*m*). Packets arriving at a node with received power greater than or equal to the *Packet Reception-Power Threshold* are received by the WLAN MAC.

The model used herein assumes: 1) zero-gain isotropic antennas so both G_{rx} *and* G_{tx} equal 1, 2) a received power threshold of -90 *dBm* (1.0×10^{-12} *W*), and 3) a 2.4 GHz WLAN center frequency which equates to $\lambda = 0.125\ m$. Given these values, the approximate transmission range is

$$r = \frac{\lambda}{4\pi} \sqrt{P_{tx} / P_{rx}} \tag{4}$$

To validate the simulated transmission ranges, a preliminary study was completed which varied P_{tx} and the distance between the sending and receiving nodes.

While the approximate range in (4) only considers path loss, the results in Table 4 for this preliminary study reflect the average transmission range during simulation and account for all modeled wireless effects. These results are used in later simulations to approximate various transmission ranges.

Table 4. Simulated Transmission Range

$P_{tx}(mW)$	Range (m)
20	1,375
25	1,530
37.5	1,900
50	2,180
75	2,680
100	3,100
150	3,800
250	4,930

A four-factor experiment with 10 replications was completed to investigate the impact that variation in routing protocol, traffic workload, transmission range, and number of nodes, has on packet delivery success and delay. Factor levels are presented in Table 5 and Table 6. Average values for each simulation are recorded for: traffic generated (*pkts/sec*), traffic received (*pkts/sec*), and end-to-end delay (*sec*).

Table 5. Experimental factor levels

Protocol	# of Nodes	Traffic Load (kbps)
OLSR	50	128
AODV	100	256
GPSR	150	512
	200	640
		1280

For comparison to GPSR, two common ad hoc routing protocols are evaluated: Optimized Link State Routing (OLSR) [11], a common proactive routing protocol, and Ad Hoc On-demand Distance Vector (AODV) [12], a popular reactive protocol. Validated and verified models for both protocols are provided with OPNET.

The simulated transmission ranges are shown in Table 6. The bold values are optimal transmission ranges determined from the Java simulation discussed in Section 2.3. For comparison, an additional set of simulations was performed with no routing and a 14.525 *km* transmission range (the longest possible distance between any two nodes).

Table 6. Transmission range factor levels

# Nodes	Approx Range (*km*)				
50	1.375	2.18	**2.68**	3.8	4.93
100		1.375	**1.90**	2.68	3.8
150		1.375	**1.53**	2.18	3.1
200			**1.375**	2.18	3.1

5. Results

Statistics from each configuration are averaged across all 10 replications. Packet delivery ratio (PDR) is compute by dividing the total number of packets delivered to all destination nodes by the total number of packets generated by all nodes. An analysis of variance (ANOVA) performed on PDR finds that all factors and interactions are statistically significant at the 0.05 significance level; variance components are presented in Table 7. The second-order interaction between number of nodes and transmission range is excluded because the two factors are covariate.

Table 7. Packet delivery rate ANOVA

Source	DF	Adj SS	% of Variance
Protocol	2	25.29	20.1%
Nodes	3	0.66	0.5%
Tx Range	7	48.95	39.0%
Workload	4	23.78	18.9%
Protocol*Nodes	6	5.87	4.7%
Protocol*Tx Range	14	1.45	1.2%
Protocol*Workload	8	4.45	3.5%
Nodes*Workload	12	0.30	0.2%
Tx Range*Workload	28	2.66	2.1%
Error	2315	12.20	9.7%
Total	2399	125.62	

Several plots are produced with 90% confidence intervals to examine the response in PDR and delay.

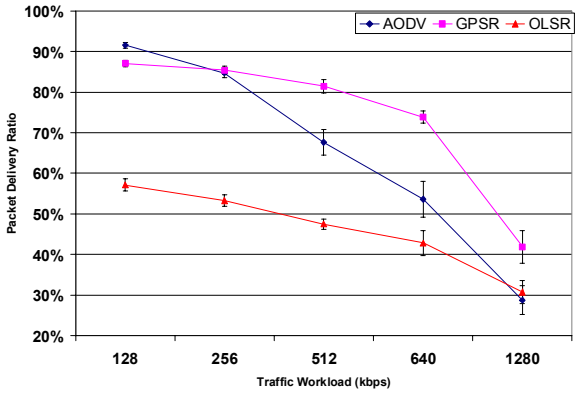

Figure 6. PDR vs traffic workload (*kbps*) for 100 nodes at optimal transmission range

Figure 6 plots PDR versus traffic workload for 100 nodes using optimal (1.9 *km*) transmission range. In all but the most lightly-loaded network, GPSR has the best PDR. Figure 7 shows PDR versus transmission range for 100 nodes with a 512 *kbps* aggregate traffic workload.

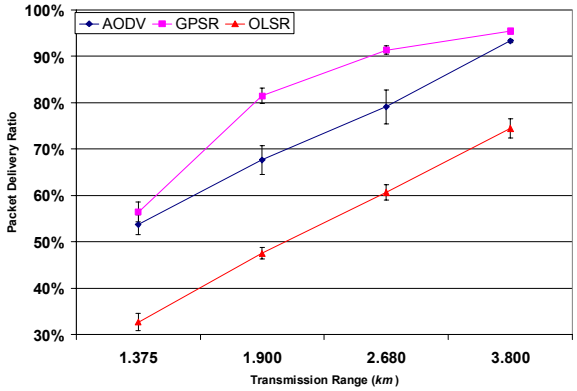

Figure 7. PDR vs transmission range (*km*) for 100 nodes at 512 *kbps* workload

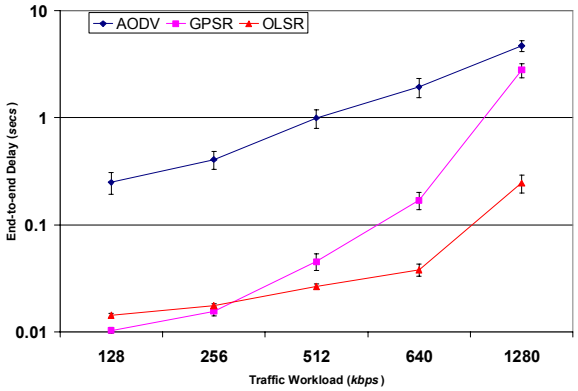

Figure 8. Delay (*secs*) vs traffic workload (*kbps*) for 100 nodes at optimal transmission range

An ANOVA is also performed for average end-to-end delay and again finds that all factors are statistically significant at the 0.05 significance level. Workload contributes the most to variation in delay, presumably due to higher channel contention requiring longer periods of transmission deferral by the WLAN MAC. Variance components are presented in Table 8. Interaction terms which include both transmission range and number of nodes are covariate and excluded from the model.

Table 8. End-to-end delay ANOVA

Source	DF	Adj SS	% of Variance
Protocol	2	197.60	4.7%
Nodes	3	113.89	2.7%
Tx Range	7	251.86	5.9%
Workload	4	1480.92	34.9%
Protocol*Nodes	6	269.02	6.3%
Protocol*Tx Range	14	332.82	7.8%
Protocol*Workload	8	111.13	2.6%
Nodes*Workload	12	210.52	5.0%
Tx Range*Workload	28	104.81	2.5%
Protocol*Nodes* Workload	24	350.52	8.3%
Protocol*Tx Range* Workload	56	321.67	7.6%
Error	2235	498.40	11.7%
Total	2399	4243.16	

In Figure 8, delay is plotted against traffic workload for a 100-node network at the optimal transmission range (1.9 *km*). Note that a log scale is used for delay due to the wide range of delay values observed.

Figure 9 is a plot of delay (using a log scale) versus transmission range for a 100-node network and 512 *kbps* traffic workload. In this case, the optimal transmission range is 1.9 *km*.

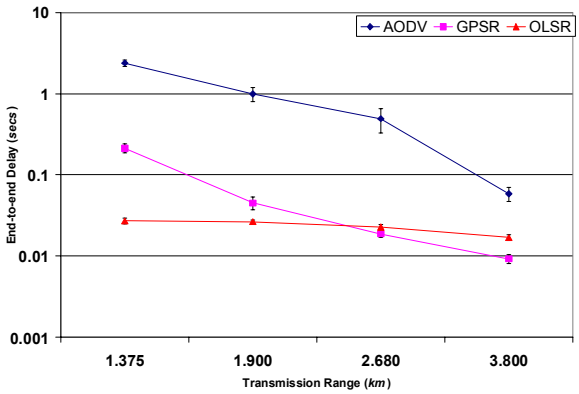

Figure 9. Delay (*secs*) vs transmission range (*km*) for 100 nodes and 512 *kbps* workload

Figure 10 plots delay versus transmission range for the highest workload configuration (200 nodes and 1280 *kbps* traffic workload). Note that a non-log scale is used for delay.

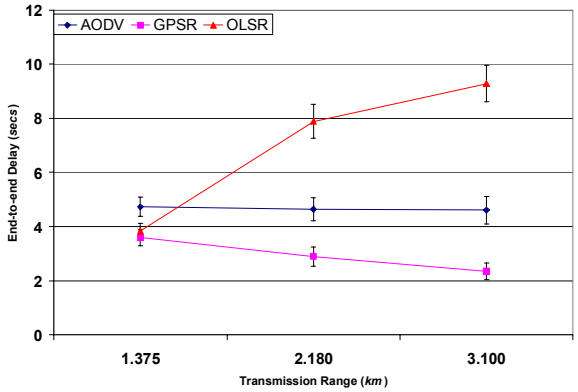

Figure 10. Delay (*secs*) vs transmission range (*km*) for 200 nodes at 1280 *kbps* workload

21st International Conference on
Advanced Information Networking and Applications Workshops (AINAW'07)
0-7695-2847-3/07 $20.00 © 2007 IEEE

These results show that as transmission range increases, OLSR appears to become overloaded and average delay increases to nearly 10 *secs*. AODV maintains a fairly constant delay as transmission range increases and GPSR experiences a decrease in delay (approximately one second) as range increases. However, even the smallest delay shown (over two seconds for GPSR at 3.1 *km* transmission range) is considered excessive in the context of average delay.

When considering only PDR, GPSR outperforms OLSR and is better than or at least nearly matches AODV in all configurations presented above. Considering average end-to-end delay, however, GPSR and OLSR have similar delay characteristics while AODV introduces considerably more delay.

6. Conclusion

The approximate transmission range in a wireless network is provided in (4) and evaluated in the context of a swarm of autonomous UAVs. Our range approximation is most accurate in networks with 100 or more nodes, due partly to near-boundary nodes being penalized since their transmission range includes space outside the network operating region. Since it was developed assuming a uniform distribution of wireless nodes, the predicted optimal transmission ranges do not guarantee a partition free network when implemented as a network of mobile nodes traveling according to a random waypoint model. Such a mobility pattern leads to a higher probability of near-center nodes and fewer near-boundary nodes [13].

Contention for the wireless channel appears to have a significant impact on packet delivery ratio, especially in larger and more highly-loaded networks. In all scenarios, GPSR outperformed AODV and OLSR protocols with respect to PDR and delay.

There are many opportunities for future work in this area. MAC-layer feedback optimization [5] could be implemented and is expected to increase the PDR achieved by GPSR. In addition, the network could be evaluated using different traffic patterns, including distributing the aggregate workload over a greater number of generating nodes (8 were used in this study). The mobility model governing node movement and the network size could also be varied and the impact of the changes investigated.

7. References

[1] C. J. Augeri and B. E. Mullins, “Harvesting Information in Distributed Sensor Networks,” Unpublished report, Air Force Institute of Technology, July 6, 2005

[2] K. M. Morris, B. E. Mullins, D. J. Pack, G. W. P. York, and R. O. Baldwin, “Impact of Limited Communications on a Cooperative Search Algorithm for Multiple UAVs,” IEEE International Conference on Networking, Sensing and Control (submitted), 2006

[3] G. W. P. York, D. J. Pack, and J. Harder. “Comparison of Cooperative Search Algorithms for Mobile RF Targets using Multiple Unmanned Aerial Vehicles.” Invited chapter in Cooperative Control and Optimization, University of Florida Press, Gainesville, 2006.

[4] M. Mauve, A. Widmer and H. Hartenstein, "A survey on position-based routing in mobile ad hoc networks," in IEEE Network, vol. 15, pp. 30-39, 2001

[5] B. Karp and H. T. Kung, "GPSR: Greedy perimeter stateless routing for wireless networks," in MobiCom '00: Proceedings of the 6th Annual International Conference on Mobile Computing and Networking, pp. 243-254, 2000

[6] G. Toussaint, “The relative neighborhood graph of a finite planar set,” in Pattern Recognition vol. 12, pp. 261-268, 1980

[7] P. Gupta and P. R. Kumar, “The capacity of wireless networks,” in IEEE Transactions on Information Theory, vol. 46, pp. 388-404, 2000

[8] F. Xue and P. R. Kumar, “The number of neighbors needed for connectivity of wireless networks,” in ACM Wireless Networks, vol. 10, no. 2, pp. 169-181, 2004

[9] Fabian Kuhn, Roger Wattenhofer, Yan Zhang and Aaron Zollinger, “Geometric Ad-Hoc Routing: Of Theory and Practice,” *22nd ACM Symposium on the Principles of Distributed Computing (PODC)*, 2003

[10] Fabian Kuhn, Roger Wattenhofer and Aaron Zollinger,”Worst-Case Optimal and Average-Case Efficient Geometric Ad-Hoc Routing,” *4th ACM International Symposium on Mobile Ad Hoc Networking and Computing (MOBIHOC)*, 2003

[11] P. Jacquet, P. Muhlethaler, T. Clausen, A. Laouiti, A. Qayyum, L. Viennot, "Optimized link state routing protocol for ad hoc networks," in *Technology for the 21st Century*, pp. 62- 68, 2001

[12] C. E. Perkins and E. M. Royer, "Ad-hoc on-demand distance vector routing," in Proceedings of the 2nd IEEE Workshop on Mobile Computing Systems and Applications, pp. 90-100, 1999

[13] T. Camp, J. Boleng and V. Davies, "A survey of mobility models for ad hoc network research," Wireless Communications and Mobile Computing, vol. 2, pp. 483-502, 2002